Autonomous Navigation for Crewed Lunar Missions with DBAN[1]

William Jun
Georgia Institute of Technology
North Ave NW
Atlanta, GA 30332
wjun7@gatech.edu

Kar-Ming Cheung
Jet Propulsion Laboratory
California Institute of Technology
4800 Oak Grove Dr.
Pasadena, CA 91109
kar-ming.cheung@jpl.nasa.gov

Julia Milton
Massachusetts Institute of Technology
77 Massachusetts Ave
Cambridge, MA 02139
jmilton@mit.edu

Glenn Lightsey
Georgia Institute of Technology
North Ave NW
Atlanta, GA 30332
glenn.lightsey@gatech.edu

Charles Lee
Jet Propulsion Laboratory
California Institute of Technology
4800 Oak Grove Dr.
Pasadena, CA 91109
charles.h.lee@jpl.nasa.gov

Abstract — **With the recent push for a crewed Lunar mission to descend, land, and ascend from the Moon, there is a need for real-time position, velocity, and orientation knowledge of a Lunar spacecraft. Proposed approaches to achieve this include the use of weak-signals received from GPS and Deep Space Network (DSN)-aided measurements, but these all require significant hardware development and active tracking from multiple ground stations. Additionally, these solutions may be unavailable during close approach and landing. This paper extends the previously published relative Doppler-based positioning scheme (Law of Cosines – LOC) and an absolute Doppler-based scheme (Conic Doppler Localization – CDL) with the aid of range measurements and an inertial measurement unit (IMU) to create the Doppler Based Autonomous Navigation (DBAN) architecture. DBAN allows for real-time, autonomous positioning with as few as one Lunar orbiter and a reference station on the surface of the Moon.**

The LOC scheme is a relative navigation architecture that converts Doppler measurements into Doppler-based range measurements with the aid of a reference station and at least one satellite. In addition, the CDL scheme is an absolute navigation architecture that converts Doppler measurements into conic sections for angle-based positioning. These schemes allow for localization with solely Doppler measurements that can be made using existing hardware, with significant performance improvements when including range measurements. However, the existing drawback with these schemes is that they require a static user; they can be biased through the Doppler shift produced by a dynamic user. However, with the aid of range measurements, an IMU, and a non-linear Kalman filter, DBAN can correct these biases and provide continuous Doppler-based navigation.

In this analysis, the Lunar Gateway and the Lunar Relay Satellite (LRS) were used with a pre-existing reference station located on the south pole of the Moon to localize a user during orbit, descent, and landing. A surface constraint assumption was optionally implemented using the knowledge of the altitude of the user as a constraint. Satellite ephemeris, velocity, and external and internal measurement errors were modeled as Gaussian variables and embedded in Monte Carlo simulations to increase fidelity. An Extended Kalman Filter (EKF) was used to ensure quick convergence without effects from linearization during intervals of high user dynamics.

Ultimately, the DBAN architecture may provide real-time positioning, velocity, and orientation knowledge with a minimal navigation infrastructure that relaxes hardware requirements and utilizes as few as one orbiter.

TABLE OF CONTENTS

1. INTRODUCTION

With the quickly approaching plans for a crewed mission to descend, land, and ascend from the Moon, there is a growing need for a navigation architecture that can be autonomous from the Earth and sustainable for the future. Some potential architectures have included the use of weak GNSS signals [1] and active tracking with the Deep Space Network (DSN) [2]. However, these and other methods like them, would require significant hardware implementations and cooperation and observables from Earth.

A new navigational architecture is introduced in this paper called Doppler Based Autonomous Navigation (DBAN). DBAN can enable real-time, autonomous positioning with as few as one Lunar orbiter and a reference station on the surface

978-1-7821-2734-7/20/$31.00 ©2020 IEEE

of the planet. Because DBAN is not reliant on Earth based observations, the user is able to calculate their own respective position. DBAN can allow for a primary or redundant navigation system if/when Earth based navigation systems fail. This can make the system useful for crewed missions.

DBAN is a system that contains inertial navigation systems, coupled with Joint Doppler and Ranging (JDR) schemes that enable both relative and absolute positioning. These are loosely integrated through an Extended Kalman Filter (EKF). The relative JDR scheme is an extension of an only Doppler based navigation scheme called the Law of Cosines (LOC). The LOC scheme is a relative navigation architecture that converts Doppler measurements into Doppler-based range measurements with the aid of a reference station and at least one satellite [3]. The absolute JDR scheme is an extension of an only Doppler based navigation scheme called Conic Doppler Localization (CDL). This scheme converts Doppler measurements into conic sections for angle-based positioning. However, the existing drawback with these schemes is that they require a static user; they can be biased through the Doppler shift produced by a moving user. However, with the aid of range measurements, an IMU, and a non-linear Kalman filter, DBAN can correct these biases and provide continuous navigation.

In this analysis, the Lunar Gateway and the Lunar Relay Satellite (LRS) were used with a pre-existing reference station located on the south pole of the Moon to localize a user during a transfer orbit and Low Lunar Orbit. The user was assumed to be the Human Landing System (HLS) undocking from the Gateway and arriving at a parking orbit of 100 km above the Lunar surface. A navigation grade inertial navigation system (INS) is utilized on the user (sampled at 10 Hz), with two way ranging and Doppler measurements made from each visible satellite (sampled at 1 Hz).

With DBAN, the positioning accuracy had approached 8 km with a maximum error of about 10 km after 13 hours of integration. This was a significant improvement from the error from dead reckoning of approximately 10,000 km. Just as with position, velocity error was also increased with an increase in user dynamics, reaching 1.5 m/s of error with a maximum of 2.3 m/s.

Ultimately, the DBAN architecture can provide real-time positioning, velocity, and orientation knowledge with significant improvements to standard dead reckoning. DBAN can enable a minimal navigation infrastructure that can enable autonomous positioning of crewed missions.

2. WORKING PRINCIPLES

Doppler and Range Based Positioning Schemes

The Law of Cosines (LOC) scheme is a relative Doppler based positioning scheme that requires a reference station and as few as one satellite to localize a user [3]. A novel algorithm is used in this scheme to convert Doppler measurements into Doppler based Range measurements. Because current proximity link radios can log Doppler shifts of locked satellites in real time, positioning is enabled with relatively low hardware requirements with LOC.

Additionally, the Conic Doppler Localization (CDL) scheme is an absolute scheme that positions by calculating intersections of multiple, infinite conics produced by Doppler measurements. Because this is an absolute scheme there is no need for a reference station. However, error from Doppler measurements and errors in satellite velocity and satellite ephemeris knowledge are directly embedded into the final position fix.

Joint Doppler and Ranging (JDR) is the addition of range measurements into both of the previously mentioned Doppler based positioning schemes. JDR with the LOC scheme, called JDR-LOC, can enable improved performance and real time localization with as few as one satellite [4]. Additionally, JDR with CDL, called Modified CDL (MCDL), can enable improved performance by limiting the length of the conics produced by the Doppler measurements. Two-way ranging and two-way Doppler measurements were assumed for this analysis.

Additionally, the knowledge of the user's altitude can be used with both of these schemes as an additional pseudorange measurement from a faux satellite at the center of the planet. This faux measurement is known as the surface constraint [4].

With DBAN, both the absolute and the relative positioning schemes are utilized. The absolute scheme (MCDL) is used by default and the relative scheme (JDR-LOC) is used when the reference station is in view and in range. Therefore, there is the constant utilization of measurements from satellites in view, with improved position fixes when the reference station is available.

Inertial Navigation Systems (INS)

One drawback of the previously mentioned positioning schemes is that they are dependent on external satellites. This reliance can lead to low update frequencies and/or signal dropouts. A solution to this is the use of an Inertial Navigation System (INS). An INS is a system of sensors that measure the relative accelerations and angular velocities of a body. The INS can integrate these measurements to calculate the relative position and orientation change of the body in 3 dimensions [5]. The INS can allow for relative positioning in a self-contained system, enabling navigation when external positioning schemes are unavailable.

In this report, the INS measurements were simulated from a given trajectory of the user, allowing for the repeated simulation of the measurements with various input error cases. A navigation grade inertial measurement unit (IMU) was assumed in this analysis.

INS/JDR Integration System

In this implementation, the INS was loosely coupled with the JDR schemes through the Extended Kalman Filter (EKF).

This meant that the position fixes created from the JDR schemes at each measurement instance were treated as direct input to the Kalman filter (Figure 1). The calculated position from the IMU was used as the nominal trajectory in the EKF.

Reference Frames

Body Frame ("BOD")—This frame has its origin aligned with the IMU, with its three axes aligned with the three most sensitive axes of the IMU. Although the body frame origin is

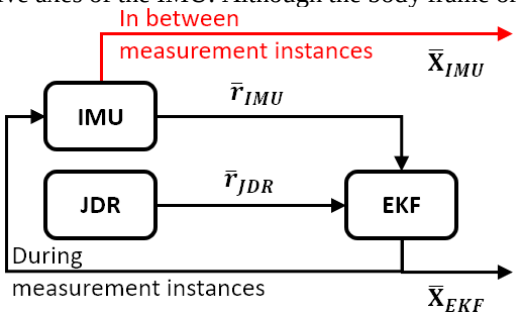

Figure 1: Block Diagram of a Loosely Coupled INS/JDR Integration. $\bar{\mathbf{r}}$ are the calculated position vectors and $\bar{\mathbf{X}}$ is the current state vector

typically set at the center of mass of the user, this body frame was aligned with the "sensor frame" of the IMU to remove the need for level arm compensation and simplify the analysis. All inertial measurements were made in the body frame. In this report, the x-axis of the body frame was aligned with the velocity vector of the user.

Fixed Frame ("FIX" – frame)—This planet fixed frame has its origin at the center of mass of the planet / planetary body with its axes rotating with respect to the body's rotation. The x-axis is typically pointing to a reference point, the z-axis is parallel to the mean spin axis of the planet, and the y-axis is orthogonal to x and z. This reference frame was used as the primary navigational frame.

3. Review of Equations

Joint Doppler and Ranging – Law of Cosines (JDR-LOC)

The Doppler based pseudorange equation for the JDR-LOC scheme can be derived assuming a nearby reference station that can communicate measurements to the user (1) [4]. $\vec{P}$ is the relative positioning vector from the reference station to the user. A description of all terms, the full derivation of this equation, and the resulting cost function is described in Appendix A. The implemented form of equation 1 was modified to move all Cosine terms into a numerator to reduce the divergent effects of dividing by zero. This form was shown for clarity.

$$\left(\frac{(\vec{L}^i + \vec{P}) \cdot \hat{u}_v^i}{cos\theta^i}\right)^2 = \left(\frac{\vec{L}^i \cdot \hat{u}_v^i}{cos\phi^i}\right)^2 + \|\vec{P}\|^2 - 2\left(\frac{\vec{L}^i \cdot \hat{u}_v^i}{cos\phi^i}\right)(\vec{P} \cdot \hat{u}^i) \quad (1)$$

Additionally, the standard range equation is utilized (without clock correction) (2).

$$PR^i = \left\|\left(\vec{L}^i + \vec{P}\right) - \vec{C}^i\right\| \quad (2)$$

Modified Conic Doppler Localization (MCDL)

Unlike the relative technique, the MCDL scheme for absolute positioning does not have independent Doppler and ranging equations. Rather, they are coupled to allow for the range measurements to actively correct the Doppler conic equations (3). $\vec{U}$ is the absolute position vector from the origin to the user. A description of all terms, the full derivation of this equation, and the resulting cost function is described in Appendix B.

$$cos\theta^i * PR^i = \left(\vec{U} - \vec{C}^i\right) \cdot \hat{u}_v^i \quad (3)$$

INS Mechanization Equations

The mechanization equations in this analysis were fairly simplistic. One reason for this was that the user was limited to only traversing over the Moon, not on its surface. This meant that many of the additional effects of planet rotation on IMU measurements did not play a factor in this analysis. Additionally, the simplicity was to quantify feasibility of the DBAN system with highly dynamic users.

Measurement Corrections—First, the raw, body frame measurements taken from the IMU were corrected for their biases. The estimated biases were taken from the current state vector.

$$\bar{a}_{BOD}^{corrected} = \bar{a}_{BOD}^{raw} - \bar{b}_{accel} \quad (4)$$

$$\bar{\omega}_{BOD/FIX}^{corrected} = \bar{\omega}_{BOD/FIX}^{raw} - \bar{b}_{gyro} \quad (5)$$

The body to fixed frame quaternion from the current state was first converted into a rotation matrix. All the measurements, which are taken in the body frame, were converted into the fixed frame using this rotation matrix.

$$R_{BOD2FIX}(\bar{q}_{BOD2FIX}) \quad (6)$$

Velocity Update—The corrected acceleration measurements in the body frame were then multiplied by the time increment to obtain velocity increments. This velocity increment was rotated into the fixed frame and combined with the previous state's velocity vector to obtain the current state's velocity.

$$\Delta t = t_k - t_{k+1} \quad (7)$$

$$\bar{v}_{FIX_k} = R_{BOD2FIX}\bar{a}_{BOD}^{corrected}\Delta t + \bar{v}_{FIX_{k-1}} \quad (8)$$

Position Update—The position was then integrated using the simple trapezoidal method (appropriate with high sampling rates).

$$\bar{r}_{FIX_k} = \frac{1}{2}\left(\bar{v}_{FIX_k} + \bar{v}_{FIX_{k-1}}\right)\Delta t + \bar{r}_{FIX_{k-1}} \quad (9)$$

Attitude Update—Finally, the attitude was updated by converting the corrected angular velocity measurements into an angular increment rotation vector:

$$\bar{\theta}_{BOD/FIX}^{increment} = \bar{\omega}_{BOD/FIX}^{corrected}\Delta t \quad (10)$$

This rotation vector was then converted into a quaternion:

$$\bar{q}_{t_{k-1}2t_k}\left(\bar{\theta}_{BOD/FIX}^{increment}\right) \quad (11)$$

Finally, the quaternion was inverted and multiplied with the quaternion from the previous state vector to obtain the current orientation.

$$\bar{q}_{BOD2FIX_k} = \bar{q}_{BOD2FIX_{k-1}} * \bar{q}_{t_{k-1}2t_k}^{-1} \quad (12)$$

Extended Kalman Filter (EKF)

To run a sequential filter, such as the EKF, there are prerequisites that must be known about the given system. These can include: the state vector, the forcing function, and measurement models. The calculated position from the IMU was utilized as the nominal trajectory in this analysis.

Estimated State—The state that was estimated in the EKF contained the user's position and velocity in the fixed frame, the user's body to fixed frame orientation in quaternions, and bias terms in three dimensions for the accelerometers and gyroscopes. Therefore, the state had a total of 16 terms:

$$\bar{\mathrm{X}} = \begin{bmatrix}\bar{r}_{FIX} & \bar{v}_{FIX} & \bar{q}_{FIX} & \bar{b}_{Gyro} & \bar{b}_{Accel}\end{bmatrix}^{\mathrm{T}} \quad (13)$$

Forcing Function—The forcing function, or the derivative of the state vector, is used to describe the dynamics of the state vector elements. It can be described as a linear combination of the state vector in the matrix A:

$$A = \begin{bmatrix}0 & V & 0 & 0 & 0\\ C & 0 & 0 & 0 & 0\\ 0 & 0 & Q & 0 & 0\\ 0 & 0 & 0 & B_a & 0\\ 0 & 0 & 0 & 0 & B_g\end{bmatrix} \quad (14)$$

Where:

$$V = I^{3x3} \quad (15)$$

$$C = \frac{\mu}{r^5}\begin{bmatrix}2x - \frac{y^2+z^2}{x} & 3x & 3x\\ 3y & -2y + \frac{x^2+z^2}{y} & 3y\\ 3z & 3z & -2z + \frac{x^2+y^2}{z}\end{bmatrix} \quad (16)$$

$$r = \sqrt{x^2+y^2+z^2}$$

$$Q = \frac{1}{2}\begin{bmatrix}0 & \omega_z & -\omega_y & \omega_z\\ -\omega_z & 0 & -\omega_x & \omega_y\\ \omega_y & -\omega_x & 0 & \omega_z\\ -\omega_x & -\omega_y & -\omega_z & 0\end{bmatrix} \quad (17)$$

$$B_a = g\begin{bmatrix}\frac{1}{\omega_z} & -\tau & 0\\ \tau & \frac{1}{\omega_z} & 0\\ 0 & 0 & 0\end{bmatrix} \quad (18)$$

$$B_g = b_g - \omega(\omega + kg)^{-1}(b_g - k_p b_a) \quad (19)$$

Finally, the matrix A was used to calculate the state transition matrix:

$$\phi(t_k, t_{k-1}) = I^{16x16} + \sum_{n=1}^{20}\frac{1}{n!}A^n(t_k - t_{k-1}) \quad (20)$$

Measurement Model—Because the input to the EKF was just the position fix calculated by either MCDL or JDR-LOC, the measurement model was simply the nominal trajectory.

$$G(\bar{\mathrm{X}}_k^*, t_k) = \bar{\mathrm{X}}_k^* \quad (21)$$

Calculating the dynamics of the measurement model:

$$\tilde{H}(\bar{\mathrm{X}}^*, t_k) = \begin{bmatrix}-1 & 0 & 0 & \\ 0 & -1 & 0 & 0^{3x13}\\ 0 & 0 & -1 & \end{bmatrix} \quad (22)$$

Finally, the standard equations for an Extended Kalman Filter are used to calculate the new state. The time update was as follows:

$$\bar{P}_k = \phi(t_k, t_{k-1})\bar{P}_{k-1}\phi^T(t_k, t_{k-1}) \quad (23)$$

The observation was then made, and the optimal gain was calculated:

$$y_k = Y_k - G(\bar{\mathrm{X}}_k^*, t_k) \quad (24)$$

$$K_k = \bar{P}_k\tilde{H}_k^T\left(\tilde{H}_k\bar{P}_k\tilde{H}_k^T + R_k\right)^{-1} \quad (25)$$

Finally, the measurement update was as follows:

$$\bar{\mathrm{X}}_k = \bar{\mathrm{X}}_k + K_k y_k \quad (26)$$

$$P_k = \left(I - K_k\tilde{H}_k\right)\bar{P}_k \quad (27)$$

4. SCENARIO

User and Satellite Trajectory

Reasonable assumptions were made for choosing the satellites that would be available during a crewed Lunar their transfer orbit. Included was the Gateway and the Lunar Relay Satellite (LRS). Access between the Human Landing System (HLS) and each satellite and the reference station were calculated. The switch between the use of either MCDL and JDR-LOC schemes was dependent on access and range between the user reference station.

Human Landing System (HLS)—The HLS was assumed to undock from the Gateway at a point past the Gateway's apolune. Once undocked, the HLS would be on a transfer orbit on route to an insertion into a 100 km parking orbit (Figure 2). The HLS is assumed be able to communicate with multiple entities simultaneously, enabling two way ranging and Doppler from multiple satellites.

Because there is an orbit maneuver in the HLS's trajectory (circularizing the transfer orbit ellipse at 100 km), it was assumed to be an instantaneous delta-V maneuver. Thus, the true velocity had a discontinuity and therefore the acceleration was extremely large at a single timestep. When simulating the accelerometer measurements this acceleration spike was kept to ultimately ensure the correct change in position.

South Pole Reference Station (REF)—The reference station was assumed to be static on the south pole of the Moon. This reference station could be anything from a simple monument to a Lunar habitat; as long as the station can receive and transmit to the satellites and the HLS. The transmitting range of the reference station was assumed to be 5000 km. Additionally, the location of the reference station was assumed to be very well known.

When the HLS had access to the reference station and was within the range of 5000 km, DBAN switched to the JDR-LOC scheme instead of MCDL.

Lunar Relay Satellite (LRS)—The LRS is an elliptical 12 hour frozen orbit around the Moon [6]. The LRS is assumed be able to communicate with multiple entities simultaneously, enabling two way ranging and Doppler on the user and the reference station.

Gateway (GTW)—The Gateway is 7 day near-rectilinear halo orbit (NRHO) around the Moon. The GTW is assumed be able to communicate with multiple entities simultaneously, enabling two way ranging and Doppler on the user and the reference station.

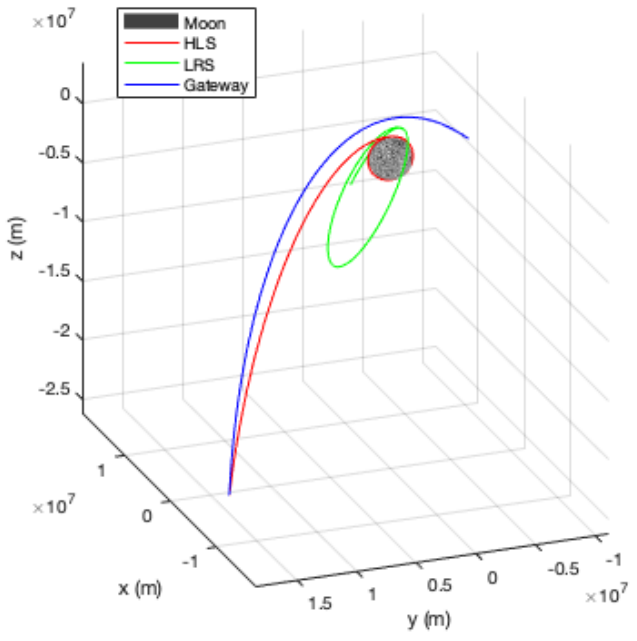

Figure 2: HLS, LRS, and Gateway Trajectories

5. Simulation Setup

Satellite ephemeris, satellite velocity, Doppler measurements, and pseudorange measurements were required in both JDR schemes. The true measurements were calculated with the true locations and velocities of each satellite and the reference station. These measurements and the satellite ephemeris and velocity were then corrupted with Gaussian error (Table 1) before their input into the JDR schemes. A new Gaussian noise value was calculated for each axis at each timestep.

Table 1: 1σ Gaussian Error Values

Error Type	Value
Satellite Ephemeris Vector (3D)	5 m
Satellite Velocity Vector (3D)	1 mm/s
Pseudorange Measurement	5 cm
Doppler Measurement	0.00075 Hz
Surface Constraint	10 m

The Doppler measurements of each communication link was calculated with a K-Band carrier frequency of $18 * 10^9$ Hz. These measurements were taken at 1 Hz; with one measurement per satellite, per second.

Simulation of IMU Data

Along with the JDR measurements, IMU measurements were required. To simulate these measurements, the derivative of the true velocity of the HLS was calculated and stored as the corresponding acceleration. Additionally, the true rotation vectors between each timestep of the body frame of the HLS were used to calculate the angular velocities. These measurements were sampled at 10 Hz.

These true accelerations and angular velocities were corrupted based off of the characteristics of a navigation grade IMU (Table 2).

Table 2: Navigation Grade IMU Parameters

Device	Parameter	Value
Gyroscope	Measurement Range	400 deg
	Resolution	0.001 deg/$\sqrt{\text{hr}}$
	Constant Bias	0.01 deg/$\sqrt{\text{hr}}$
	Random Walk	0.005 deg/$\sqrt{\text{hr}}$
Accelerometer	Measurement Range	10 g
	Resolution	50e-6 g
	Constant Bias	500e-6 g
	Noise Density	10e-6 g/$\sqrt{\text{hr}}$

6. Results

With all of the corrupted measurements and satellite data ready, the simulation was performed with the DBAN architecture. Due to the stochastic nature of the simulation there exist variations in results. Including a Monte Carlo analysis to create a distribution of error is dictated in future work.

A baseline error was created by running the simulation without the JDR schemes. This preliminary run was therefore performed with dead reckoning – only reliant on the IMU measurements. This was depicted in gray in the Log plots (Figure 3 and 4).

Position Error

After using DBAN to propagate and actively filter approximately 13 hours of integration, the final positioning error was approximately 8 km (Figure 3). Although this may seem like a large amount, it is miniscule compared to the baseline error of approximately 10,000 km.

Also described at the top of Figure 3 is the timeline of satellite and reference station access vs. use of absolute or relative JDR schemes throughout DBAN. The utilization of JDR-LOC is short in this case due to the limited transmission range of the reference station. However, the JDR-LOC scheme would be heavily used during and after landing.

The start of the first orbit was aligned with a significant jump in positioning error. This was due to the simultaneous loss of sustained satellite access and a dynamic change to a new orbit. However, once the filter had become accustomed to the new dynamics, the error began to fall. Additionally, error was further decreased during intervals utilizing JDR-LOC.

Velocity Error

Again, it was clear that DBAN had outperformed dead reckoning by multiple orders of magnitude (Figure 4). However, there was an spike in the velocity error at the start of hour 12. This was due to the discontinuity in velocity that was caused by the simplifications in orbit maneuvers (discussed in "4. Scenario").

7. CONCLUSIONS

With an IMU sampling rate of 10 Hz and a measurement instance rate of 1 Hz over 13 hours of integration, the DBAN system was able to maintain errors under 10 km. For the first 10 hours, errors were consistently under 1 km, implying that continuous use of DBAN over multiple orbits without maneuvers would decrease error. The velocity error was also consistently under 2.5 m/s, with a spike at 12 hours that was caused by simplifications in the simulation (instantaneous delta-v for orbit insertion. However, just as with the position error, velocity errors were under 0.3 m/s for the first 10 hours. Ultimately, both were significant improvements over the extreme errors caused by simple dead reckoning.

An area of improvement could be the use of directional antennas with the reference station. This would allow for a larger range for the reference station and therefore a larger utilization of the JDR-LOC scheme. Additionally, because this is still only in the simulation world, the epoch of the LRS could be moved to allow for increased access during highly dynamic maneuvers such as circularization of the transfer orbit.

Only the HLS's transfer orbit and one low Lunar orbit was

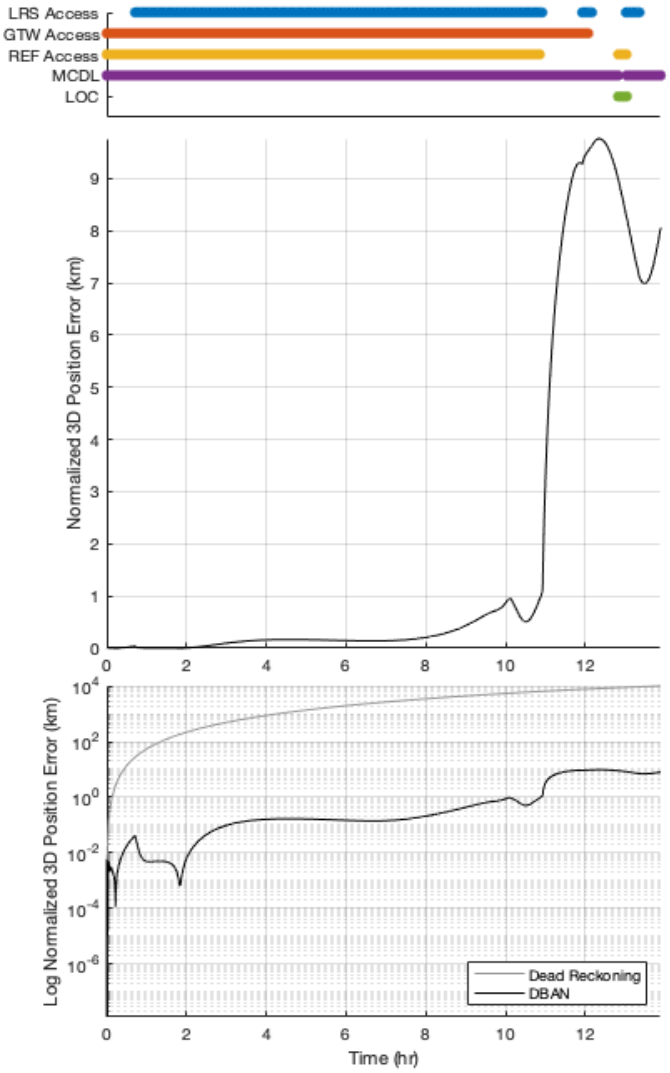

Figure 3: Position Error Over Transfer and Orbit

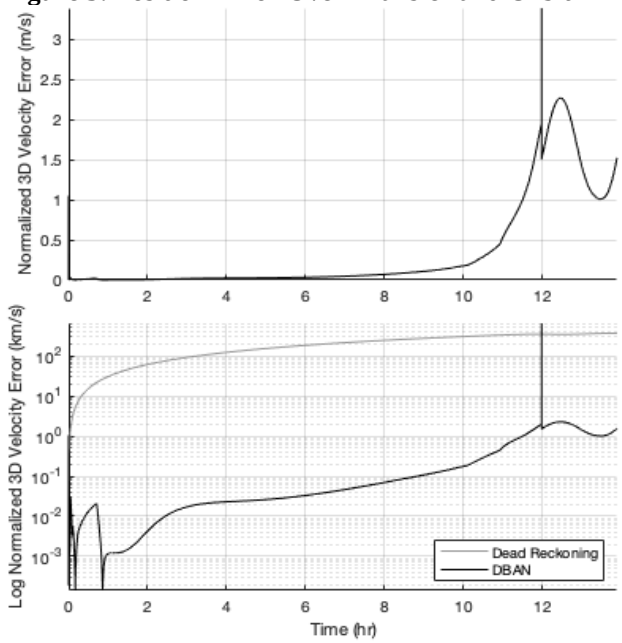

Figure 4: Velocity Error Over Transfer and Orbit

included in this analysis. Future work would include DBAN with the descent and landing onto the Lunar surface. Although users on the surface of the Moon have already been analyzed in previous work [3,4], it would be interesting to apply the entire DBAN system on relatively slowly moving surface users.

Additionally, a Monte Carlo analysis would allow for a distribution of potential error, displaying all of the biases of the stochastic simulation. Finally, improved error modelling of the IMU would allow for accurate inertial measurements, while also increasing the state size. A trade will need to be performed to find the correct balance between them.

Although this analysis was completed with the Moon, which has many possibilities for potential navigation architectures from Earth, DBAN could also be applied to other planets that do not have any navigational infrastructures. In a standard exploratory mission, a lander could be sent with an orbiter, undock from a parking orbit and land on the surface. Then, a rover could roll off of the lander and explore the region. With all of these components, the DBAN architecture would allow for accurate positioning throughout the entire EDL and surface navigation process. Ultimately, the DBAN system can be applied to a myriad of space-based navigation needs that require autonomous positioning with limited resources.

APPENDICES

A. JDR-LOC DERIVATION

The JDR-LOC scheme is a modification of the original LOC scheme including ranging measurements in addition to Doppler measurements [4]. A review of the JDR-LOC scheme was provided. The visualization of the user (T), the reference station (R), and one of the satellites (C) is described in Figure 5.

$$\vec{L}^{i\prime} = \begin{bmatrix} l_1^i \\ l_2^i \\ l_3^i \end{bmatrix} \quad \hat{u}_v^i = \begin{bmatrix} v_1^i \\ v_2^i \\ v_3^i \end{bmatrix}$$

$$\hat{u}^i = \begin{bmatrix} u_1^i \\ u_2^i \\ u_3^i \end{bmatrix} \quad \vec{P} = \begin{bmatrix} x \\ y \\ z \end{bmatrix}$$

$$\vec{X} = \begin{bmatrix} \vec{P} \\ ct \end{bmatrix} \quad R = \begin{bmatrix} r_1 \\ r_2 \\ r_3 \end{bmatrix}$$

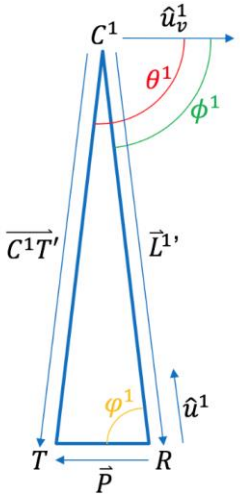

Figure 5: Visualization of the LOC Technique $\hat{u}_v^i$ is the satellite's velocity vector, R is the reference station, T is the user, and C^1 is the current satellite

Using the Law of Cosines, a cost function can be created (28). This is the core cost function of the LOC scheme; the relative position P can be calculated from the other input measurements.

$$f^i(x,y,z) = \left(\frac{\vec{L}^i \cdot \hat{u}_v^i}{cos\phi^i}\right)^2 + \|\vec{P}\|^2 - 2\left(\frac{\vec{L}^i \cdot \hat{u}_v^i}{cos\phi^i}\right)(\vec{P} \cdot \hat{u}^i) - \left(\frac{(\vec{L}^i + \vec{P}) \cdot \hat{u}_v^i}{cos\theta^i}\right)^2 \quad (28)$$

Additionally, the pseudorange measurement's equation is described as follows:

$$f^{i+n}(x,y,z) = \sqrt{\left((x+r_1)-c_1^i\right)^2 + \left((y+r_2)-c_2^i\right)^2 + \left((z+r_3)-c_3^i\right)^2} - PR^i \quad (29)$$

Where PR is the current satellite's pseudorange measurement. For the case of two satellites, or n = 2:

$$Calculated\ Range = CR^i = \sqrt{\left((x+r_1)-c_1^i\right)^2 + \left((y+r_2)-c_2^i\right)^2 + \left((z+r_3)-c_3^i\right)^2} \quad (30)$$

$$J(x,y,z) = \begin{bmatrix} \frac{\partial f_1}{\partial x} & \frac{\partial f_1}{\partial y} & \frac{\partial f_1}{\partial z} & 0 \\ \frac{\partial f_2}{\partial x} & \frac{\partial f_2}{\partial y} & \frac{\partial f_2}{\partial z} & 0 \\ \frac{(x+r_1)-c_1^1}{CR^1} & \frac{(y+r_2)-c_2^1}{CR^1} & \frac{(z+r_3)-c_3^1}{CR^1} & 1 \\ \frac{(x+r_1)-c_1^2}{CR^2} & \frac{(y+r_2)-c_2^2}{CR^2} & \frac{(z+r_3)-c_3^2}{CR^2} & 1 \end{bmatrix} \quad (31)$$

Finally, the surface constraint equation is as follows:

$$SC = surface\ constraint$$
$$f^{i+2n}(x,y,z) = (x+r_1)^2 + (y+r_2)^2 + (z+r_3)^2 - SC * SC \quad (32)$$

And the respective updated cost functions and Jacobians with only two satellites (n = 2):

$$f(x,y,z) \quad (33)$$

$$J(x,y,z) \quad (34)$$

$$f(x,y,z)=\begin{bmatrix}\left(\frac{\vec{L}^1\cdot\hat{u}_v^1}{cos\phi^1}\right)^2+\|\vec{P}\|^2-2\left(\frac{\vec{L}^1\cdot\hat{u}_v^1}{cos\phi^1}\right)(\vec{P}\cdot\hat{u}^1)-\left(\frac{(\vec{L}^1+\vec{P})\cdot\hat{u}_v^1}{cos\theta^1}\right)^2\\ \left(\frac{\vec{L}^2\cdot\hat{u}_v^2}{cos\phi^2}\right)^2+\|\vec{P}\|^2-2\left(\frac{\vec{L}^2\cdot\hat{u}_v^2}{cos\phi^2}\right)(\vec{P}\cdot\hat{u}^2)-\left(\frac{(\vec{L}^2+\vec{P})\cdot\hat{u}_v^2}{cos\theta^2}\right)^2\\ \sqrt{\left((x+r_1)-c_1^1\right)^2+\left((y+r_2)-c_2^1\right)^2+\left((z+r_3)-c_3^1\right)^2}+ct-PR^1\\ \sqrt{\left((x+r_1)-c_1^2\right)^2+\left((y+r_2)-c_2^2\right)^2+\left((z+r_3)-c_3^2\right)^2}+ct-PR^2\\ (x+r_1)^2+(y+r_2)^2+(z+r_3)^2-SC^2\end{bmatrix},\quad J(x,y,z)=\begin{bmatrix}\frac{\partial f_1}{\partial x}&\frac{\partial f_1}{\partial y}&\frac{\partial f_1}{\partial z}&0\\ \frac{\partial f_2}{\partial x}&\frac{\partial f_2}{\partial y}&\frac{\partial f_2}{\partial z}&0\\ \frac{(x+r_1)-c_1^1}{CR^1}&\frac{(y+r_2)-c_2^1}{CR^1}&\frac{(z+r_3)-c_3^1}{CR^1}&1\\ \frac{(x+r_1)-c_1^2}{CR^2}&\frac{(y+r_2)-c_2^2}{CR^2}&\frac{(z+r_3)-c_3^2}{CR^2}&1\\ 2(x+r_1)&2(y+r_2)&2(z+r_3)&0\end{bmatrix}$$

B. MCDL Derivation

The MCDL scheme is a modification of the original CDL scheme including ranging measurements in addition to Doppler measurements.

The doppler count measurement along with the transmitted frequency can be used to solve for the range rate of the satellite, where *a* is the line of sight between the satellite and the user.

$$DopplerCount = f_{received} - f_{transmitted} \tag{35}$$

$$f_{received} = f_{transmitted}\left(1 - \frac{V_{sat}^i \cdot \hat{V}_a^i}{c}\right) \tag{36}$$

$$RangeRate = -c * \frac{DopplerCount}{f_{transmitted}} \tag{37}$$

This range rate, along with the satellite's velocity vector, can be used to calculate the angle between the satellite's velocity vector and the line of sight vector from the satellite to the user:

$$RangeRate = proj_{\hat{a}_i} V_{sat}^i = \|\hat{a}_i\| * \left\|V_{sat}^i\right\| cos\theta \tag{38}$$

$$cos\theta = -\frac{RangeRate}{\left\|V_{sat}^i\right\|} \tag{39}$$

Knowing this angle, the equation of the infinite, circular cone describing all possible solutions for the user's location can be derived:

$$cos\theta^i = \frac{\bar{U} - \bar{C}^i}{\|\bar{U} - \bar{C}^i\|} \cdot \hat{u}_v^i \tag{40}$$

Because a pseudorange measurement is also made, it can replace the term $\|U - S\|$. It is assumed that the two way ranging can lead to no clock correction term. With the user's cartesian location as U, the satellite's cartesian location as S, the satellite's cartesian velocity unit vector as $\hat{u}_v^i$, and the pseudorange measurement as PR the final equation for one measurement's circular cone of solutions with the length of the pseudorange can be derived:

$$cos\theta^i * PR^i = \left(\vec{U} - \vec{C^i}\right) \cdot \hat{u}_v^i \tag{41}$$

Acknowledgements

The research described in this paper was carried out at the Jet Propulsion Laboratory, California Institute of Technology, under a contract with the National Aeronautics and Space Administration. The research was supported by NASA's Space Communication and Navigation (SCaN) Program.

This work was additionally supported by a NASA Space Technology Research Fellowship.

References

[1] M. Manzano-Jurado, J. Alegre-Rubio, A. Pellacani, et al., "Use of weak GNSS signals in a mission to the moon", 2014 7th ESA Workshop on Satellite Navigation Technologies and European Workshop on GNSS Signals and Signal Processing (NAVITEC). Noordwijk, Netherlands, 2014.

[2] J. M. Leonard, J. S. Parker, R. L. Anderson, et al., "Supporting crewed lunar exploration with LiAISON navigation," 36th Annual Guidance and Control Conference. Breckenridge, Colorado. 2013.

[3] K. Cheung, W. W. Jun, C. Lee, E. G. Lightsey, "Single-Satellite Doppler Localization with Law of Cosines (LOC)," 2019 IEEE Aerospace Conference, Big Sky, MT, 2019.

[4] K. Cheung, W. W. Jun, E. G. Lightsey, C. Lee, T. Stevenson, "Single-Satellite Real-Time Relative Localization Using Joint Doppler and Ranging (JDR)", 70th International Astronautical Congress 2019, October 2019.

[5] A. O. Salytcheva, "Medium accuracy INS/GPS integration in various GPS environments," Master thesis, University of Calgary, UCGE Reports Number 20200. 2004.

[6] S. R. Oleson, M. L. McGuire, "COMPASS Final Report: Lunar Relay Satellite (LRS)", NASA/TM-2012-217140

BIOGRAPHY

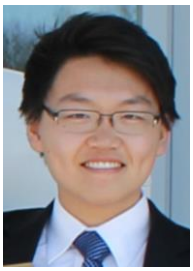

William Jun *received a BS in Aerospace Engineering from the Georgia Institute of Technology in Atlanta, GA. Over the course of his time at Georgia Tech, he has worked in the Space Systems Design Laboratory (SSDL) on various CubeSat missions as subsystem leads and as the Project Manager of Prox-1. He started his work in navigation architectures during an internship at the NASA Jet Propulsion Laboratory over the summer of 2018. He is currently continuing his education with a PhD at Georgia Tech, working under Dr. Glenn Lightsey.*

Kar-Ming Cheung *is a Principal Engineer and Technical Group Supervisor in the Communication Architectures and Research Section (332) at JPL. His group supports design and specification of future deep-space and near-Earth communication systems and architectures. Kar-Ming Cheung received NASA's Exceptional Service Medal for his work on Galileo's onboard image compression scheme. Since 1987, he has been with JPL where he is involved in research, development, production, operation, and management of advanced channel coding, source coding, synchronization, image restoration, and communication analysis schemes. He got his B.S.E.E. degree from the University of Michigan, Ann Arbor, in 1984, and his M.S. and Ph.D. degrees from California Institute of Technology in 1985 and 1987, respectively.*

Julia Milton *received her B.S. in Industrial and Operations Engineering (2014) from the University of Michigan. She is currently working on a M.S. in Technology and Policy and a PhD in Aeronautics and Astronautics at the Massachusetts Institute of Technology. As a member of the Engineering Systems Laboratory, her main areas of research are methods for designing and analyzing complex socio-technical systems that involve a mix of architecture, technologies, policy issues and complex networked operations.*

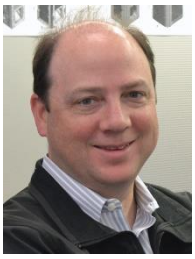

E. Glenn Lightsey *is a Professor in the Daniel Guggenheim School of Aerospace Engineering at the Georgia Institute of Technology. He is the Director of the Space Systems Design Lab at Georgia Tech. He previously worked at the University of Texas at Austin and NASA's Goddard Space Flight Center. His research program focuses on the technology of satellites, including: guidance, navigation, and control systems; attitude determination and control; formation flying, satellite swarms, and satellite networks; cooperative control; proximity operations and unmanned spacecraft rendezvous; space based Global Positioning System receivers; radionavigation; visual navigation; propulsion; satellite operations; and space systems engineering. At the University of Texas, he founded and directed the Texas Spacecraft Lab which built university satellites. He has written more than 130 technical publications. He is an AIAA Fellow, and he serves as Associate Editor-in-Chief of the Journal of Small Satellites and Associate Editor of the AIAA Journal of Spacecraft and Rockets.*

Professor Charles H. Lee *received his Doctor of Philosophy degree in Applied Mathematics in 1996 from the University of California at Irvine. He then spent three years as a Post-Doctorate Fellow at the Center for Research in Scientific Computation, Raleigh, North Carolina, where he was the recipient of the 1997-1999 National Science Foundation Industrial Post-Doctorate Fellowship. He became an Assistant Professor of Applied Mathematics at the California State University Fullerton in 1999, Associate Professor in 2005, and since 2011 he has been a Full Professor. Dr. Lee has been collaborating with scientists and engineers at NASA Jet Propulsion Laboratory since 2000. His research has been Computational Applied Mathematics with emphases in Aerospace Engineering, Telecommunications, Acoustic, Biomedical Engineering and Bioinformatics. He has published over 65 professionally refereed articles. Dr. Lee received Outstanding Paper Awards from the International Congress on Biological and Medical Engineering in 2002 and the International Conference on Computer Graphics and Digital Image Processing in 2017. Dr. Lee also received NASA's Exceptional Public Achievement Medal in 2018 for the Development of his Innovative Tools to Assess the Communications & Architectures Performance of the Mars Relay Network.*